J. Membrane Biol. 75, 193–203 (1983)

The Journal of
Membrane Biology

Localization of Ionic Pathways in the Teleost Opercular Membrane by Extracellular Recording with a Vibrating Probe

Carl Scheffey*, J. Kevin Foskett** and Terry E. Machen

Departments of Physiology-Anatomy and Zoology, and Cancer Research Laboratory, University of California, Berkeley, California

Summary. We have adapted the vibrating probe extracellular recording technique to use on an epithelium under voltage clamp in an Ussing chamber. The vibrating probe allows very low drift measurements of current density immediately over the epithelial surface. These measurements allowed sites of electrogenic transport in the epithelium to be localized with a spatial resolution of 5 μm. The technique was applied to the opercular membrane of the teleost fish, the tilapia, *Sarotherodon mossambicus*. The mitochondrion-rich "chloride cells" were shown to be the only sites of electrogenic ion transport in this heterogeneous epithelium. Cell sampling experiments demonstrated variable negative short-circuit currents associated with nearly all of approximately 300 chloride cells examined, which appeared to account for all of the tissue short-circuit current. Current-voltage relations for individual cells were also measured. Conductance associated with chloride cells (i.e. cellular and junctional pathways) accounted for all but 0.5 mS/cm^2 of the tissue conductance, with the balance apparently accounted for by leak pathways near the edge of the tissue. Current and conductance associated with other cell types was at least 50-fold smaller than for the chloride cell. Chloride-free solutions reduced chloride cell current and conductance by 98 and 95 %, respectively.

Key Words: vibrating probe · chloride cell · teleost opercular membrane · extracellular recording · tilapia

Introduction

Since its introduction (by Ussing, 1949), the Ussing chamber has been a workhorse of epithelial physiology. The technique can measure flux or current across the whole tissue, but has the disadvantage that the pathways for transport are not immediately known. For heterogeneous epithelia, it is desirable to know which cell types are involved in the transport. Several recent approaches to this problem have included selective collection of tracers crossing the epithelium from different locations on the epithelium (Jarrell, King & Mills, 1981), correlation of changes in physiology and/or transport with the structure and/or number of a specific cell type (e.g. Rosen, Oliver & Steinmetz, 1974; Mills & Malick, 1978; Voûte & Meier, 1978; Wade, O'Neil, Pryor & Boulpaep, 1979; Marshall & Nishioka, 1980; Stetson, Wade & Giebisch, 1980; Bobrycki, Mills, Macknight & DiBona, 1981; DiBona et al., 1981; Foskett et al., 1981; Husted, Mueller, Kessel & Steinmetz, 1981), histochemical and chemical localization of specific enzymes to specific cell types (e.g. Scott, Sapirstein & Yoder, 1974; Husted et al., 1981; Narbaitz, Kacew & Sitwell, 1981), culture of individual cell types (*see* Handler, Perkins & Johnson, 1980), and binding of agents to specific cell types (e.g. Lettir, Kaissling, Koeppen & Wade, 1982). Pathways for electrogenic transport across an epithelium can also be localized by the purely electrical approach of measuring the distribution of extracellular current density immediately above the epithelium (Frömter, 1972; Frömter & Diamond, 1972; Hudspeth, 1975; Cereijido, Stefani & Palomo, 1980). The present study took the extracellular recording approach using the vibrating probe for measuring current density, a technique that has not previously been applied to voltage-clamped epithelia but which is especially well-suited to measuring steady extracellular current.

The vibrating probe has been successfully used to measure steady ionic currents in a variety of biological preparations (Jaffe & Nuccitelli, 1977; Jaffe, 1981). The tip of a metal microelectrode is vibrated back and forth along a line 5 to 30 μm long. If a voltage field is present along that line, the movement of the microelectrode causes the voltage of the mi-

* *Present address:* National Vibrating Probe Facility, Marine Biological Laboratory, Woods Hole, Mass. 02543.
** *Present address:* Laboratory of Kidney and Electrolyte Metabolism, National Heart, Lung and Blood Institute, National Institutes of Health, Bethesda, Md. 20205.

croelectrode to oscillate. These oscillations can be analyzed to yield a measurement of the electric field along the line of vibration. The technique has less noise than other means of measuring extracellular fields because it virtually eliminates the noise contribution of the electrode tip.

We have adapted the vibrating probe technique to measure the distribution of current flow through a flat sheet epithelium, the teleost opercular membrane. Although the opercular membrane is comprised of several cell types (Foskett et al., 1981), a variety of indirect evidence has indicated that one cell type in this membrane, the chloride cell, is responsible for its electrogenic transport (reviewed by Karnaky, 1980, and by Foskett, Bern, Machen & Connor, 1983). We recently reported (Foskett & Scheffey, 1982) direct evidence that this is indeed the case for opercular membranes from seawater-adapted tilapia, using the vibrating probe technique.

For the present study, we have further refined the application of vibrating probe for use on flat-sheet epithelia. We describe here (1) an improvement in spatial resolution that enabled us to better address questions about the ionic pathways of the opercular membrane, and (2) details of the technique and experiments that illustrate some of its advantages and limitations.

Materials and Methods

Animals and Dissection

Tilapia, *Sarotherodon mossambicus*, were maintained and dissected as previously described (Foskett et al., 1981). Fish were maintained in freshwater and adapted to seawater for 14 to 40 days prior to experiments. Opercular membranes were removed, and the connective tissue on the serosal side of the membranes was teased away using fine forceps.

Experimental Chamber and Solutions

The isolated opercular membranes were mounted in a modified Ussing chamber that allowed continuous perfusion of both sides of the tissues with oxygenated Ringer's solution. The Ringer's solution contained the following (in mM): Na^+, 160; Cl^-, 151; HCO_3^-, 15; K^+, 3; Ca^{++}, 2; PO_4^{--}, 1; Mg^{++}, 1; SO_4^{--}, 1; Tris(hydroxymethyl)-aminomethane$^+$, 5; glucose, 10. The Ringer's was titrated with H_2SO_4 to a pH of 7.9 when gassed with a 99% O_2/1% CO_2 mixture. For some experiments, a chloride-free Ringer's was used that substituted 4 mM gluconate and 147 mM isethionate for chloride ions.

Membranes were mounted horizontally across a circular aperture (area = 0.516 cm^2) with the apical side up. Each membrane was supported on a nylon mesh (Nytex HC3-209) and stretched between pins around the aperture. Silicon grease (Dow) was smeared above and below the tissue around the edge of the aperture as a sealant, and a thin annular Lucite® chip was pressed down over the tissue around the edge of the aperture. This chip was made only 1/32″ thick, to allow the shank of the vibrating electrode to approach the tissue from as nearly a horizontal direction as possible. Experiments were carried out under observation by an upright, fixed-stage microscope with Nomarski optics (Aus Jena) utilizing 32× (Leitz) and 10× (Zeiss) objectives with working distances 6 and 4.8 mm, respectively. Details of the experimental chamber and optics will be described in a future communication.

A commercial voltage-clamp circuit was used employing series resistance compensation (Model 710C, Bioengineering Division, College of Medicine, University of Iowa). Transepithelial potential was measured by calomel electrodes connected to the tissue by agar bridges that ended near its two sides. Current was passed by chlorided silver wires on either side of the tissue. The current-passing electrode on the apical side was held near ground by a virtual ground circuit contained in the voltage clamp.

Vibrating Probe: Construction and Noise

The vibrating probe extracellular recording technique was a modification of that described by Jaffe and Nuccitelli (1974).

The metal electrode to be vibrated was constructed as follows. A borosilicate glass microelectrode was pulled on a standard microelectrode puller. The electrode was cut 2 cm from the tip to leave a short glass funnel, and the tip was broken off to a diameter of 1 to 2 μm by touching it to a microscope slide under microscopic observation. Wood's metal (Fisher) to be used in filling the electrode was prepared by melting and sucking it into a silastic tube to form a wire. The wire was inserted into the back end of the funnel, which was then rested on a bar heated to 80 °C to melt the Wood's metal. A wire that closely fit into the back end of the funnel was used to push the melted metal up to the tip. Electrical contact was made to the back end of the Wood's metal by melting it there and inserting a 125 μm gold wire. The other end of the gold wire was connected via a coaxial cable with driven shield to one input of a differential preamplifier (described below) that allowed measurement of electrode capacitance.

As an optional step that may help to keep the electrode's capacitance stable, the tip could be gold plated at this stage. The tip was placed in 0.2% AuKCN. If a ball of Wood's metal had formed at the tip, it was broken off by tapping the electrode. The metal tip was gold plated under microscopic observation by passing current into the tip from a platinum electrode also in the AuKCN solution: 0.05 μA for 5 min and then 0.2 μA until a gold ball of about 2 μm was formed. Tip capacitance was checked after gold plating; an anomalously high capacitance was taken as evidence that the glass wall had broken near the tip. The tip was next rinsed in distilled water, and platinized under microscopic observation using a protocol similar to that of Jaffe and Nuccitelli (1974). The procedure could be used to easily construct electrodes with tip diameters as small as 3 μm. Tips of diameter 4 to 6 μm with capacitances of 0.3 to 1 nF were used in the present study.

The mechanical power to vibrate the electrode was provided by a piezoelectric bimorph (PZT-5HN, Vernitron Piezoelectric Division, Bedford, Ohio). The bimorph

was contained in a grounded metal box and one side of it was grounded. A 2 cm long glass rod was epoxied to the grounded side and passed through a hole in the box; the electrode was waxed to the other end of the rod. The ungrounded side of the bimorph was powered with a sine wave of up to 20 V peak-to-peak at a resonant frequency near 1.6 kHz, allowing the electrode tip to be vibrated along a line up to 20 μm long. We shall refer to the length of this line of vibration as the "probe excursion," and its center as the "center of excursion." Probe excursions of 4 to 7 μm were used in the present study.

The voltage signal of the tip was measured with respect to a chlorided silver wire near the tip in the bath by a differential preamplifier near the preparation whose input capacitance was 20 pF and whose input noise density was under 6 $nV/Hz^{1/2}$ at the frequency of vibration. The preamplifier contained switching circuitry that allowed the vibrating tip to be connected to a variable current source, for electroplating. The tip could also be connected through a 12 pF capacitor to a 6 mV amplitude triangle wave, for the purpose of measuring tip capacitance and convergence resistance. The triangle wave source then passed a square wave of current into the tip, resulting in a tip signal that was the sum of a square wave of amplitude proportional to tip convergence resistance and a triangle wave inversely proportional to tip capacitance. Those tip parameters could then be measured by observing the tip voltage signal while the triangle wave was applied. This arrangement served to monitor the tip capacitance during platinization. Tip capacitance and convergence resistance were also checked during experiments, in order to make sure the tip had not fractured or accumulated excessive debris.

The tip voltage signal from the preamplifier was processed by a lock-in amplifier, which multiplied into the tip signal a sine wave of the vibration frequency whose phase was adjusted to that of the tip vibration, so that the sine wave reached its maximum as the tip excursion reached its extreme (*cf.* Jaffe & Nuccitelli, 1974). The product was then filtered one-pole with a time constant of 0.1 to 0.66 sec, to provide the output of the lock-in amplifier. The output is then proportional to an average of the electric field along the line of tip vibration, and response to changes in the field with a time constant equal to that of the output filter.

The electronics to implement the above operations were based on a quadrature oscillator integrated circuit (Burr-Brown 4423). Its sine and cosine outputs were added with a variable weighting and rescaled to provide one sine wave to power the piezoelectric element and another of variable relative phase to be multiplied into the vibrating electrode signal.

The theoretically attainable minimum noise for a vibrating probe measurement of current density is given in Appendix A. In practice, actual current noise was within a factor of 2 of the theoretical minimum, typically 1 $\mu A/cm^2$ rms.

Vibrating Probe: Calibration

The vibration of the electrode tip vigorously stirred the nearby solution, creating fluid velocities exceeding 0.1 mm/sec that could be observed as particles in the solution passed the tip. Because of this stirring, it was assumed that the resistivity of the Ringer's near the vibrating probe was the same as the bulk Ringer's resistivity, even when the probe was located near the membrane surface, when ion or water transport might alter the local resistivity in the absence of stirring. With that assumption, lock-in output is proportional to the current density in the line of vibration. Lock-in outputs are then reported in this paper as current densities. The constant of proportionality between the lock-in output and the electric field in the direction of vibration was determined empirically. The vibrating probe was positioned in the experimental chamber in the geometry used in experiments, and the chamber was filled with Ringer's to the depth used in experiments. Pulses of measured current were passed from a microelectrode that was moved around in the plane 100 μm above the probe to find the position giving the maximal probe response. This occurred when the line from the probe to the microelectrode had a direction halfway between vertical and the direction of probe vibration. The current density in the direction of probe vibration created by the current from the microelectrode could be calculated, whose ratio with the probe response yielded the desired conversion factor from probe signal to current density.

The above geometry was used for probe calibration because it mimicked the geometry used to measure the current pumped by a chloride cell, when the probe was positioned over the cell to obtain the maximum probe signal. By using the same geometry for both measurements, the estimate of current pumped by the cell was insensitive to error in estimating the direction of probe vibration, which could not be directly observed during the nearly vertical vibration.

For measurements conducted in chloride-free Ringer's the conversion factor from probe signal to current density was obtained by multiplying the conversion factor for normal Ringer's by 0.6, the empirically determined ratio between the conductivities of the two Ringer's.

The conversion factor from probe signal to current density at the tip could also be calculated by estimating the probe excursion visually and calculating an expected conversion factor from the gain of the lock-in amplifier. The calculated conversion factor usually agreed with the conversion factor obtained empirically. For some electrode tips, the empirical conversion factor gave less probe signal than calculated per current density. This was taken as evidence of electrical leakage in the shank of the electrode, and it was discarded.

The current pumped by a chloride cell crypt was quantitatively estimated using the assumptions (justified below) that all the current passed though the apical crypt of the chloride cell and that the surrounding apical surface may be considered as an insulating boundary. The estimate for current pumped by the cell was

$$I = \frac{FC}{2}\left(\frac{h}{H}\right)^2 \frac{V_1}{V_2} \tag{1}$$

where V_1 = probe signal measured over the cell, V_2 = probe response during the calibration procedure to passing current C from the microelectrode, h = height of the center of the probe excursion above the opening of the apical crypt, H = height of current-passing electrode above the probe during the calibration (typically 100 μm), and F is a correction factor of 0.96 to 1.0.

The factor F was calculated to correct for the experiment's departure from an idealized geometry. Although this correction turned out to be quite small, its calculation is described in detail in Appendix B because the considerations involved are likely to be important in some other vibrating probe applications.

Grounding

Extreme caution was necessary in the electronic grounding scheme. Grounding arrangements that would be acceptable for most other kinds of extracellular recording could introduce sub-microvolt signals at the probe input that caused probe output signal artifacts. There were no ground loops. Connections between grounding wires were designed to have reliably low resistance. Grounding of circuits that carried high level signals of vibration frequency was kept separate from grounding of the voltage-clamp and vibrating probe preamplifier circuits. Digital noise had to be kept out of the voltage-clamp command potential and away from the preparation, because the high frequency noise picked up at the probe's input could create low frequency noise at the lock-in amplifier output. Electrostatic shielding and other customary precautions were used to minimize noise of power line frequency in the vibrating electrode signal, which could create noise below 1 Hz at the lock-in amplifier output.

Results

Localization of Electrogenic Current Sources and Estimation of Their Size

Figure 1 shows current density measurements (closed circles) made by the probe as it moved along a line of points 8 μm above the apical surface passing over the apical crypt shared by two chloride cells. (Most crypts were associated with only one chloride cell, but a few percent were associated with two or even three chloride cells.) The data of this Figure were collected under voltage clamp at short-circuit conditions. The probe reports negative current coming out of the epithelium in the vicinity of chloride cells. Peak current density occurs at the apical crypt; the density decreases to half of the peak when the probe is 5 μm from the crypt and to under 3 % when it is 30 μm away.

The open circles in Fig. 1 show calculated theoretical current densities based on the assumption that all the current coming through the local epithelium was coming through the apical crypt of the chloride cell. These calculations were numerical integrations similar to that described in Appendix B.

Similar peaks of current were observed over all but two of the nearly three hundred chloride cell crypts that were approached with the probe in 9 opercular membranes. The peak of current density always occurred nearly directly above the crypt of the cell. (Because the vibration of the probe was not quite vertical, the maximum current density would be recorded 1 to 3 μm away from directly above the center of the crypt, on the assumption that all the current

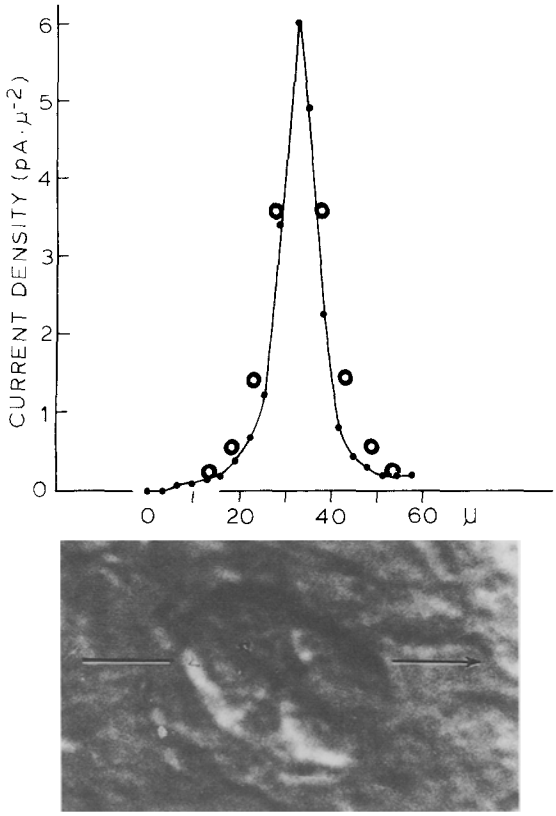

Fig. 1. Vibrating probe measurements of current density around an apical crypt. Photo shows path of the probe over the apical crypt, which appears as a small crater between two chloride cells. Negative current density leaving the epithelium (pA/μm², ordinate, solid dots) is plotted against probe position (abscissa, marked in μm immediately over probe positions in the photo). (1 pA/μm² = 100 μA/cm².) Open circles show theoretical calculated current densities, normalized to coincide with the data at the peak over the crypt

was coming from the crypt.) No other peaks of current density were observed on the tissue surface.

When the probe was more than 50 μm away from a chloride cell, the current density was near zero (less than 3 μA/cm²). If no chloride cell was within 150 μm of the probe, the current density was indistinguishable from zero. This consistent drop-off to zero current density was not obtained in our previous study (Foskett & Scheffey, 1982).

The better rejection of distant current sources in the present study was obtained by using smaller vibrating probe tips, and vibrating closer to the epithelial surface in a more closely vertical direction. The importance of these factors is explained in Appendix C.

In the present study, the height of the probe's center of excursion above the tissue was

7 to 15 μm, and the vibration excursion was 4 to 7 μm, in a direction 20° from vertical. There were practical limitations on how much rejection of distant current sources could be improved by adjusting these parameters. The direction of vibration could not be closer to vertical because of the geometry of the experimental chamber. Electrode tip diameter could not be made too small because of the resultant increase in probe signal noise (*see* Appendix A). The probe was not operated any closer to the tissue primarily because this made the uncertainty in the estimate (1) too great. The fixed uncertainty in estimating the height above the tissue became a larger fraction of the total height, increasing the uncertainty in the estimate (1), which is proportional to h^2.

A nonzero current density of up to 3 μA/cm^2 was often measured away from a chloride cell, but it could always be accounted for as current spread from the chloride cells in the area (*see* Appendix C). The data above are consistent, then, with the hypothesis that all of the short-circuit current passes through the apical crypts of chloride cells. If some of the short-circuit current passes through other cells away from chloride cells, then the density of that current must be under 3 μA/cm^2, compared with a typical total membrane short-circuit current density in the present study of 30 to 50 μA/cm^2.

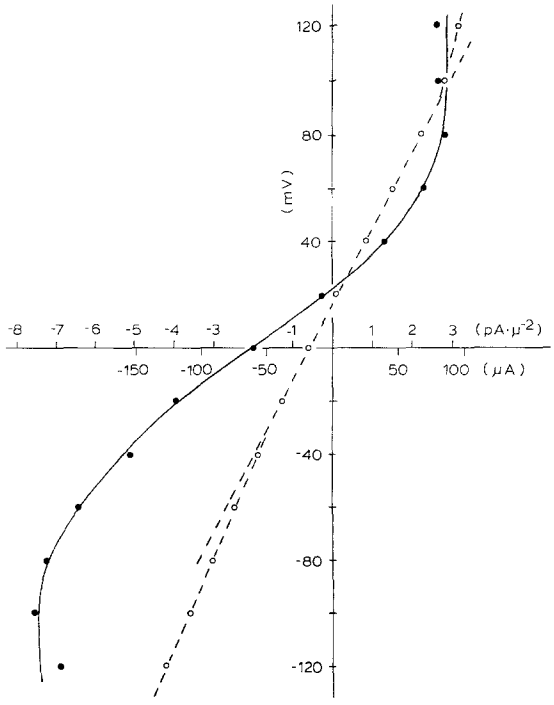

Fig. 2. Current-voltage relations for chloride cell and whole opercular membrane. Transepithelial voltage (mV, ordinate) is plotted against transepithelial current (μA, open circles connected by dotted lines) and current density over single chloride cell (pA/μm^2, solid dots connected by solid line)

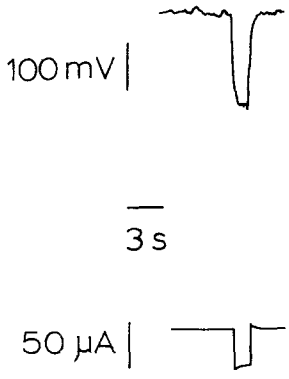

Fig. 3. Vibrating probe recording over a chloride cell during a voltage step. Transepithelial potential was clamped to zero, stepped to +40 mV for 1.5 sec, and then returned to zero. Upper trace, vibrating probe signal. (A 100 mV signal corresponded to a current density of 1.15 pA/μm^2.) Lower trace, transepithelial current

The Current-Voltage Relationship of Chloride Cells

In addition to locating sources of transepithelial current, the vibrating probe can measure current-voltage relations for individual sources. For the experiment shown in Fig. 2, the vibrating probe was located 18 μm above a chloride cell crypt, and the lock-in amplifier output filter time constant was set at 0.24 sec. The transepithelial potential was held at zero and stepped momentarily to various voltages. A transient artifact sometimes appeared in the probe signal at the start of the voltage step (*see below*), but this artifact always settled to a negligible value within 1/2 sec. Figure 2 plots the total transepithelial currents and probe-reported current densities recorded at one second into the voltage steps. Figure 3 shows an example of the vibrating probe output during a voltage step. The current-voltage relation reported by the probe is that for the crypt and its vicinity, including any paracellular pathways associated with the crypt.

The transient artifact that can appear in the probe signal at the start of a voltage step also occurs when the probe is far from a chloride cell. (The artifact was not large enough to be apparent in Fig. 3.) The artifact can occur be-

Table 1. Cell sampling experiments[a]

Exp. no.	Cl cells/cm^2 ($\times 10^{-4}$)	Sum I_{sc} of cells (μA/cm^2)	I_{sc} (μA/cm^2)	% I_{sc} accounted for	Sum G of cells (mS/cm^2)	G_t (mS/cm^2)	% G_t accounted for
1.	1.34	34.2	40.7	84	2.29	2.98	76
2.	0.69	23.9	32.9	73	0.68	1.78	38
3.	0.48	7.6	19.4	39	0.16	0.70	23
4.	1.34	24.4	31.0	79	1.24	1.94	64
5.	0.80	14.8	17.4	85	0.47	0.70	67
6.	1.23	51.6	32.9	157	0.84	1.05	80
7.	1.03	24.4	36.8	66	0.68	1.26	54
8.	1.62	30.2	36.8	82	0.48	1.13	43
9.	1.32	47.0	50.3	93	2.04	2.56	80
means				84			58

[a] Shown are chloride cell density ("Cl cells/cm^2"), probe-estimated sum of cells' short-circuit currents ("sum I_{sc} of cells"), whole tissue I_{sc}, % I_{sc} accounted for, estimated sum of cells' conductances ("sum G of cells"), whole tissue conductance (G_t), and % G_t accounted for.

cause the transient voltages at current passing electrodes and the transient current passing in the chamber at the time of the voltage step cause a voltage transient in the vibrating electrode tip that is large compared with the submicrovolt signals that are involved in the current density measurements.

The chloride cell current-voltage relationship of Fig. 2 is typical of 8 chloride cells examined. It is linear over the range -20 (± 3 SE) mV to $+69$ (± 8 SE) mV with decreasing slope conductance for more positive and more negative potentials. The apparent transepithelial conductance in the linear range for the chloride cell of Fig. 2 was 0.2 μS, or about 3 S/cm^2 referred to the area of the crypt opening.

As we have previously reported (Foskett & Scheffey, 1982), the membrane away from chloride cells has much less conductance, less than 0.1 mS/cm^2. This is an upper bound, since the currents recorded are in part due to current from chloride cells, just as the short-circuit current density recorded away from chloride cells is in part chloride cell current.

Cell Sampling Experiments

If all of the short-circuit current is indeed pumped by chloride cells through their apical crypts, then it should be possible to sum up the currents estimated by the probe for the population of crypts and arrive at a sum equal to the total transepithelial short-circuit current. Such an estimate was made for nine tissues using the following procedure. Each tissue was divided into square 209 μm by 209 μm sections by the boundaries formed by the supporting nylon mesh. For a random sample of 12 ± 2 of these sections, the short-circuit currents and conductances of most or all the chloride cell crypts in each section were measured ($\bar{x} = 33 \pm 2$ crypts sampled in each tissue). Currents were estimated as above using Eq. (1). Conductances were measured by observing the change in the cell's current for a step to $+20$ mV, as for the current-voltage relations above, to obtain a slope conductance for the linear region of the cells' current-voltage relations. For 54 ± 9 randomly selected sections, the total number of chloride cells in each section was counted, to give an average number of cells per section, and so an estimate for the total number of cells in the area of the membrane in the Ussing chamber. When choosing areas of the tissue for cell counting and current determinations, care was taken to spread the chosen areas out evenly over the tissue, because regions of the tissue may have higher chloride cell densities than others (Foskett et al., 1981). The product of the estimated total number of cells by the estimated average current per chloride cell gave an estimated total current pumped through the chloride cells of the tissue. An estimate for the total conductance through chloride cells was similarly calculated.

The results are shown in Table 1. On the average, 84 % (± 9 % SE), or all but 4 ± 1 μA/cm^2 of the total short-circuit current was accounted for as current through the chloride cells. Because of the uncertainties in the

Table 2. Chloride-free Ringer's experiments[a]

	Short-circuit current		Conductance	
	Control	Cl^--free	Control	Cl^--free
Individual cells	2.6 ± 0.6 nA/cell	0.04 ± 0.01 nA/cell	111 ± 30 nS/cell	16 ± 3 nS/cell
Whole epithelium	61 $\mu A/cm^2$	4.8 $\mu A/cm^2$	2.06 mS/cm^2	1.16 mS/cm^2

[a] Data for individual cells shows the mean and standard error for a population of six cells.

measurements (*see* Discussion), this value is consistent with the hypothesis that all the short-circuit current is carried by chloride cells. The possible reasons for the large differences between the short-circuit current and the estimated total current of chloride cells in experiments 3 and 6 of Table 1 are discussed below. The data indicate that the total conductance associated with chloride cells is less than the total measured transepithelial conductance. This point is also discussed below.

Effects of Chloride-Free Solutions

It has been shown that the short-circuit current of opercular membranes from seawater-adapted tilapia is carried exclusively as chloride ions (Foskett et al., 1981; Foskett, Machen & Bern, 1982). If the current measured by the probe over chloride cells represents active chloride transport across the epithelium, then it should be abolished by removing chloride from both sides of the tissue. Table 2 shows the results of an experiment which verified that prediction. An epithelium was held at short-circuit conditions throughout the experiment. The probe was used to measure the currents and conductances of six chloride cell crypts while bathed in normal chloride-containing Ringer's solution. The perfusate on both sides of the membrane was then switched to a chloride-free Ringer's that substituted 147 mM isethionate and 4 mM gluconate. 35 min later, when the tissue short-circuit current and conductance had reached steady-state values of 8 and 56% of their original values, the average current measured over the same six chloride cell crypts had declined to 1.5% of its original value, and the average conductance associated with these same chloride cells had declined to 14.5% of its original value.

Discussion

This study confirms our previous finding that chloride cells are localized sites of short-circuit current across opercular membranes. The vibrating probe measurements do not directly rule out the possibility that there may be up to $3\,\mu A/cm^2$ short-circuit current passing through some areas of the epithelial surface away from the chloride cells. This uncertainty results from a limitation on the vibrating probe's ability to reject out distant current sources in the geometry of our experiments.

The cell sampling experiments were a further effort to test the hypothesis that all of the opercular membrane's electrogenic transport is associated with chloride cells. Unfortunately, using the probe to make a quantitative estimate of current through a population of cells suffers from some significant uncertainties. If two estimates were made one after the other of the current transported by a single cell, the two estimates usually agreed within 10%. There was, however, the possibility of systematic error in the optical estimation of the probe height above the apical crypt. It was difficult to focus on the rim of the crypt, and a consistent error of only 1 μm in the height estimates would have biased the cell current estimates by about 15%.

Another difficulty in estimating the total current through the chloride cell population of a tissue was that the currents pumped by individual chloride cells were highly variable and decidedly not normally distributed (manuscript in preparation). Many cells pumped ten times as much as others. The currents of a very large population of cells then had to be measured in order to obtain a reasonable estimate of the average current pumped by a cell. The density of chloride cells in different areas of the tissue was also highly variable, possibly introducing error into the estimate for the total number of chloride cells in a given tissue.

Recently we have discovered that on occasion the probe conversion factor (from lock-in output voltage to extracellular current density) could change during an experiment. Since this factor was only checked once during each cell sampling experiment, it is possible that such changes accounted for the egregious results of experiment nos. 3 and 6 of Table 1.

Taking into account these uncertainties, we regard the results of the cell sampling experiments as consistent with the hypothesis that all

of the short-circuit current in the membranes was associated with chloride cells.

Most of the transepithelial conductance is also localized to chloride cells, but a portion of it appears to be due to either edge damage or to conductance through elements of the membrane away from chloride cells. Indications of the conductance away from chloride cells are: (i) an average 0.58 mS/cm^2 of whole tissue transepithelial conductance is unaccounted for as conductance localized to chloride cells, and (ii) the reversal potential for chloride cell current was consistently more positive than the reversal potential for the whole tissue. The very low conductances (<0.1 mS/cm^2) measured with the probe over pavement cells indicate that the unaccounted-for conductance probably is not conductance through the epithelium *per se*, but instead is primarily an edge leak conductance. This hypothesis is supported by experiments on opercular membranes from freshwater tilapia, which lack differentiated chloride cells and do not actively transport chloride (Foskett et al., 1981). When these membranes are mounted in vertical Ussing chambers different from the chamber used in the present study, tissue conductance varies between 0.14 mS/cm^2 (M. Connor, B. Hughes and K. Foskett, *unpublished*) and 0.27 mS/cm^2 (Foskett et al., 1981). However, when five of the freshwater opercular membranes were mounted in the horizontal chamber used in the present study, the average conductance was 0.83 mS/cm^2, indicating an unfortunate artifactual leak conductance of 0.5 to 0.7 mS/cm^2. The magnitude of this artifactual leak conductance is close to the conductance not accounted for by chloride cells in the cell sampling experiments. In support of the artifactual nature of this conductance, (i) the probe-measured conductances for the pavement cells in the freshwater tissues were similarly low as those for seawater tissues, and (ii) using the probe on these freshwater tissues, a leak conductance was found to be associated with the edge of the aperture opening. While we have not used the probe to quantify this edge-associated conductance, it is possible to do so.

Even though this leak conductance is small, it can become an appreciable fraction of the total apparent transepithelial conductance in low conductance tissues, which are relatively sparse in chloride cells. Since the $I-V$ relation of the leak is linear, the apparent $I-V$ relation for the whole tissue can be shaped somewhat differently from the distinctly nonlinear $I-V$ relation for chloride cell crypts, as for the tissue in Fig. 2. Membranes with more chloride cells (and thus more chloride cell-associated conductance) have $I-V$ relations closer to that of chloride cells (i.e., *see* Fig. 3 in Foskett et al., 1981).

The experiments using chloride-free medium show that most of the short-circuit current and the majority, but not all, of the transepithelial conductance at a chloride cell is dependent upon the presence of chloride in the Ringer's.

The vibrating probe technique should prove useful for measuring currents pumped by single cells in other epithelia. Two major difficulties encountered in the present study may be important to setting the limitations of the probe in other flat-sheet epithelial studies. First, the optics are important in determining the spatial resolution that the probe can attain. For best spatial resolution, the probe must come as close as possible to the tissue. However, damage can occur if the probe comes too close. Good optics are required to make this compromise well. Further, as the height of the probe above the tissue is decreased, the optical uncertainty in estimating that height becomes an increasingly dominant source of error in estimating the size of current sources on the epithelial surface. The optical system must therefore have good vertical resolution (optical sectioning capability) while maintaining a relatively long working distance between the tissue and the objective to allow interposition of the probe.

A second problem of the present study will also occur in other flat-sheet epithelia: the spatial resolution required to make *quantitative* estimates of the current pumped by individual cells is far greater than the resolution required to localize *qualitatively* peaks of current density over cells. For example, in our preliminary studies on the opercular membrane, we used the probe at heights of 25 to 35 μm above the tissue. This allowed less spatial resolution than in the experiments reported above. It was possible to show peaks of current density localized to chloride cells, but the current density measured away from chloride cells was up to half the peak current density measured over chloride cells. This "background" current density was the sum of currents from all the chloride cells in the area. Quantification of the current from an individual chloride cell was then not

readily possible, since half the current density measured over a cell was current from other cells. In the present study, the probe was positioned close enough to the tissue to make the "background" current density negligible compared with the current density measured over individual cells, so that the currents of individual cells could be directly measured. Similar spatial resolution considerations will obviously pertain to other epithelia. The probe noise did not contribute appreciatively to our error in measuring the currents from individual cells. It will, then, be possible to use the probe with smaller tip diameters and smaller excursions, while maintaining the ability to quantify current sources. Whether this will result in better spatial resolution will depend on whether one's optics and preparation allow one to operate the probe significantly closer to the tissue than in the present study.

We thank Dr. Kenneth Spring for a critical reading of this manuscript. Dr. Howard A. Bern provided valuable advice and encouragement throughout the course of this study. This investigation was aided by N.S.F. grant PCM-7725205 and by P.H.S. grant CA-09041, awarded by the National Cancer Institute, D.H.H.S.

References

Bobrycki, V.A., Mills, J.W., Macknight, A.D.C., DiBona, D.R. 1981. Structural responses to voltage clamping in the toad urinary bladder. I. The principal role of granular cells in the active transport of sodium. *J. Membrane Biol.* **60**:21–33

Cereijido, M., Stefani, E., Martinez-Palomo, A. 1980. Occluding junctions in a cultured transporting epithelium: Structural and functional heterogeneity. *J. Membrane Biol.* **53**:19–32

Davenport, W.B. 1970. Probability and Random Processes. p. 518. McGraw-Hill, New York

DiBona, D.R., Sherman, B., Bobrycki, V.A., Mills, J.W., Macknight, A.D.C. 1981. Structural response to voltage-clamping in the toad urinary bladder. II. Granular cells and the natriferic action of vasopressin. *J. Membrane Biol.* **60**:35–44

Foskett, J.K., Bern, H.A., Machen, T.E., Connor, M. 1983. Chloride cells and the hormonal control of teleost fish osmoregulation. *J. Exp. Biol. Rev.* **5**:*(in press)*

Foskett, J.K., Logsdon, D., Turner, T., Machen, T.E., Bern, H.A. 1981. Differentiation of the chloride extrusion mechanism during seawater adaptation of a teleost fish, the cichlid *Sarotherodon mossambicus*. *J. Exp. Biol.* **93**:209–224

Foskett, J.K., Machen, T.E., Bern, H.A. 1982. Chloride secretion and conductance of teleost opercular membrane: Effects of prolactin. *Am. J. Physiol.* **242**:R380–R389

Foskett, J.K., Scheffey, C. 1982. The chloride cell: Definitive identification as the salt-secretory cell in teleosts. *Science* **215**:164–166

Frömter, E. 1972. The route of passive ion movement through the epithelium of *Necturus* gallbladder. *J. Membrane Biol.* **8**:259–301

Frömter, E., Diamond, J. 1972. Route of passive ion permeation in epithelia. *Nature, New Biol.* **235**:9–13

Handler, J.S., Perkins, F.M., Johnson, J.P. 1980. Studies of renal cell function using cell culture techniques. *Am. J. Physiol.* **238**:F1–F9

Hudspeth, A.J. 1975. Establishment of tight junctions between epithelial cells. *Proc. Natl. Acad. Sci. USA* **72**:2711–2713

Husted, R.F., Mueller, A.L., Kessel, R.G., Steinmetz, P.R. 1981. Surface characteristics of carbonic-anhydrase-rich cells in the turtle urinary bladder. *Kidney Int.* **19**:491–502

Jaffe, L.F. 1981. Control of development by steady ionic currents. *Fed. Proc.* **40**:125–127

Jaffe, L.F., Nuccitelli, R. 1974. An ultrasensitive vibrating probe for measuring steady extracellular currents. *J. Cell Biol.* **63**:614–628

Jaffe, L.F., Nuccitelli, R. 1977. Electrical controls of development. *Annu. Rev. Biophys. Bioeng.* **6**:445–476

Jarrell, J.A., King, J.G., Mills, J.W. 1981. A scanning micropipette molecule microscope. *Science* **211**:277–279

Karnaky, K.J. 1980. Ion-secreting epithelia: Chloride cells in the head region of *Fundulus heteroclitus*. *Am. J. Physiol.* **238**:R185–R198

Lettir, M., Kaissling, B., Koeppen, B.M., Wade, J.B. 1982. Binding of peanut lectin to specific epithelial cell types in kidney. *Am. J. Physiol.* **242**:C117–C120

Marshall, W.S., Nishioka, R.S. 1980. Relation of mitochondria-rich chloride cells to active chloride transport in the skin of a marine teleost. *J. Exp. Zool.* **214**:147–188

Mills, J.W., Malick, L.E. 1978. Mucosal surface morphology of the toad urinary bladder. Scanning electron microscope study of the natriferic and hydro-osmotic response to vasopressin. *J. Cell Biol.* **77**:598–610

Narbaitz, R., Kacew, S., Sitwell, L. 1981. Carbonic anhydrase activity in the chick embryo chorioallantois: Regional distribution and vitamin D regulation. *J. Embryol. Exp. Morphol.* **65**:127–137

Rosen, S., Oliver, J.A., Steinmetz, P.R. 1974. Urinary acidification and carbonic anhydrase distribution in bladders of Dominican and Columbian toads. *J. Membrane Biol.* **15**:193–205

Scott, W.N., Sapirstein, V.S., Yoder, M.J. 1974. Partition of tissue functions in epithelia: Localization of enzymes in "mitochondrion-rich" cells of toad urinary bladder. *Science* **184**:797–800

Stetson, D.L., Wade, J.B., Giebisch, G. 1980. Morphologic alterations in the rat medullary collecting duct following potassium depletion. *Kidney Int.* **17**:45–56

Ussing, H.H. 1949. The active ion transport through the isolated frog skin in the light of tracer studies. *Acta Physiol. Scand.* **17**:1–17

Voûte, C.L., Meier, W. 1978. The mitochondria-rich cell of frog skin as hormone-sensitive "shunt-path." *J. Membrane Biol.* **Special Issue**:151–165

Wade, J.B., O'Neil, R.G., Pryor, J.L., Boulpaep, E.L. 1979. Modulation of cell membrane area in renal collecting tubule by corticosteroid hormones. *J. Cell Biol.* **81**:439–445

Received 19 August 1982; revised 1 March 1983

Appendix A

Attainable Noise of the Vibrating Probe

The main source of the probe's noise in the present study was in practice found to be the thermal noise of the metal electrode's convergence resistance. This Appendix will derive an expression for the root mean square noise level of the probe due to this thermal noise. We use the following notation

ε = probe excursion (cm),
f_v = frequency of vibration (Hz),
H = the (complex) transfer function of the output (averaging) stage of the lock-in,
k = Boltzman constant (joule/°C),
r = effective radius of the platinized metal electrode tip (cm),
R_a = convergence resistance of the electrode, the resistance in the Ringer's between the electrode tip surface and ground (ohms),
s = rms probe current noise (A/cm^2),
σ = medium conductivity (S/cm),
T = Ringer's absolute temperature (° Kelvin), and
τ = time constant of the lock-in output stage.

The Nyquist theorem tells us that the thermal noise of the electrode's convergence resistance has a two-sided spectral density, in V^2/Hz, of

$$S_a(f) = 2kTR_a. \tag{A-1}$$

$S_a(f)$ may be related to the noise it creates at the lock-in amplifier output by paralleling the derivation on p. 518 of Davenport (1970) to give

$$s^2 = \frac{8\sigma^2}{\varepsilon^2} \int_0^\infty S_a(f)|H(f-f_v)|^2 df. \tag{A-2}$$

Using the excellent approximation

$$\int_0^\infty |H(f-f_v)|^2 df \doteq 2\int_0^\infty |H(f)|^2 df = \frac{1}{2\tau}, \tag{A-3}$$

we have

$$s^2 \doteq \frac{\sigma^2}{\varepsilon^2}\frac{8kTR_a}{\tau} \tag{A-4}$$

or

$$s \doteq \frac{6\times 10^{-11}}{\varepsilon}\sqrt{\frac{\sigma}{r\tau}}. \tag{A-5}$$

Typically for our experiments, $\tau = 0.66$ sec, $r = 3\times 10^{-4}$ cm, $\varepsilon = 5\times 10^{-4}$ cm, and $\sigma = 1.7\times 10^{-2}$ S/cm, for a minimum rms current noise of 1 μA/cm^2 or 0.01 pA/μm^2.

The above derivation is valid only for a lock-in amplifier that multiplies a sine wave into the electrode signal. *Cf.* the incorrect Eqs. (10) and (11) of Jaffe and Nuccitelli (1974), which were supposed to give attainable noise when the lock-in amplifier multiplies a square wave into the electrode signal. The correct expression for attainable rms noise in that situation is 1.11 times the expression in our Eq. (A-5). Nuccitelli reports (personal communication) that the related empirical data of their Fig. 8 (*ibid.*) was misscaled; their actual attained rms noise levels were 2.83 times larger than those shown in the Figure. They were, then, close to the theoretically attainable noise, which is also larger than they reported.

Appendix B

Explanation of Correction Factor for Crypt Current Measurement

Equation (1) without a correction factor would be precisely correct for idealized experimental geometry. Specifically, Eq. (1) would be precise with $F = 1$ if the crypt were a point source of current on an insulating plane epithelial surface, if the excursion of the probe were smaller compared with its height above the tissue, and if presence of the probe did not alter the electrical field (by a blocking action). Initial estimates indicated that the blocking action of the probe was the smallest of these errors, so a factor F was calculated to correct for the other two.

The idealization of the crypt as a point source of current was improved upon by making it a disk-shaped uniform source of current (diameter of disk = 3 μm). The electrical field generated by such a source was evaluated numerically.

The other aspect of the correction factor calculated had to do with the finite excursion of the probe tip, which moved through a line above the crypt where the voltage field was not uniform. The current density reported by the probe could not then be calculated simply as the current density at the center of probe excursion. Instead, the potentials that would be measured by the electrode as it vibrated over one cycle were taken from the numeric calculation of the field created by the disk-shaped source of current used to represent the crypt. Those measured electrode potentials were then multiplied by a sine wave in phase with the electrode motion, performing the calculation of the lock-in amplifier. The integral of these products yielded the probe response.

It turned out that these two aspects of the correction factor tended to offset each other and were both less than 10% (smaller than the probable error created by estimating the probe height above the tissue; *see* Discussion). For a typical probe excursion of 5 μm, the calculations gave correction factor (F) values of 0.96 for probe height 8 μm above the tissue, 0.97 for 10 μm, 0.98 for 12 μm, and 0.99 for height 20 μm.

It should be noted that even these "corrected" calculations make some idealizations that might need to be reconsidered for vibrating probe measurements in other situations. The electrode tip size was taken as negligibly small; it is actually large enough to disturb the electrical field to some degree and effectively average the potential on its surface rather than measure the potential at a point. The model of the crypt as a uniform disk source of current is not strictly accurate either.

Appendix C

Rejection of Distant Current Sources on the Epithelial Surface

This Appendix describes the influence of the probe's excursion, height above the tissue, and direction of vibration on the rejection of distant current sources. Denote by θ the angle from vertical of the probe's line of vibration. When $\theta > 0$ (it was 20° in the present study), the contribution of a distant current source to the probe's signal depends on the direction on the epithelial surface from the

probe to the current source. Consider first the direction from which a given current source gives a maximal contribution to the probe signal (rejection is worst). Then the contribution of the distant current source, expressed as a fraction of the signal the same source would produce if located directly under the probe (positioned for maximal response there), is

$$\left[\frac{h^3}{d^3}\cos\theta+\frac{h^2}{d^2}\sin\theta\right]\frac{1}{\cos^3\left(\frac{\theta}{2}\right)}$$

where h is the height of the probe above the tissue, and d is the distance on the epithelial surface from the probe to the current source. For example, a chloride cell pumping 1 nA of current located 70 μm away from the probe (in the worst direction) could create a probe signal equivalent to 2.5 μA/cm^2 (assuming a typical h of 15 μm).

At a direction perpendicular to that worst case direction, the expression becomes

$$\left[\frac{h^3}{d^3}\cos\theta\right]\frac{1}{\cos^3\left(\frac{\theta}{2}\right)}.$$

The above expressions are approximate and are not valid for current sources close to the probe ($d<3h$). Their close inspection should convince the reader that h and θ must be minimized in order to best reject distant sources. Probe excursion and tip size must be small as a consequence of minimizing h.

Note Added in Proof

Optical estimates of probe height, made by focusing between tissue and probe tip, were corrected for the medium's refractive index.